

Research Article

Effects of Prepolymerization, Temperature, and Hydrogen Concentration on Kinetics of Propylene Bulk Polymerization Using a Commercial Ziegler-Natta Catalyst

Huiyue Liu , Gaiping Du, Yafeng Du, Dezhan Li, and Jiangbo Chen 

SINOPEC Beijing Research Institute of Chemical Industry, Beijing 100013, China

Correspondence should be addressed to Jiangbo Chen; chenjb.bjhy@sinopec.com

Received 26 May 2022; Accepted 1 August 2022; Published 10 October 2022

Academic Editor: Kai Guo

Copyright © 2022 Huiyue Liu et al. This is an open access article distributed under the Creative Commons Attribution License, which permits unrestricted use, distribution, and reproduction in any medium, provided the original work is properly cited.

The effects of prepolymerization, temperature, and hydrogen concentration on propylene bulk polymerization with a commercial Ziegler-Natta catalyst were investigated, and the apparent polymerization rate constants were estimated by varying reaction temperatures, hydrogen partial pressures, and polymerization methods. It was shown that prepolymerization has different effects on the polymerization rate and isotacticity of the polymer; without prepolymerization, the polymerization rate and isotacticity reach their maximum at 70°C and 80°C, respectively, whereas the polymerization rate and isotacticity with prepolymerization increase with the polymerization temperature in the range of 50-80°C. Moderate prepolymerization time reduced the fine fraction while increasing polymerization rate and isotacticity. Appropriate prepolymerization technique can increase mass transfer performance and fragmentation, which is a promising way to improve polymerization rate, isotacticity index, and fine fraction. Otherwise, insufficient prepolymerization or excessive prepolymerization causes prepolymer particle fragmentation.

1. Introduction

During the initial stage of propylene polymerization, the polymer morphology was very difficult to control due to high polymerization rate; as a result, some problems like polymer powders breakage or polymer agglomeration happened, which were disadvantageous for the plant production. For these problems, catalyst prepolymerization, as a common and effective solution, was used to control the polymerization rates and get better control of polymer particle morphology before the catalyst was added into the reactors [1, 2]. The prepolymerized catalyst exhibited relatively mild polymerization rates in the reactors; thus, fragmentation of the polymer particles was controlled and less fine formed.

Many researchers have studied the effects of prepolymerization on propylene polymerization kinetics and powder particle morphology. Pater et al. [3, 4] found that the polymerization rate increased as they raised the prepolymerization temperature for propylene bulk polymerization. In another work, Pater

et al. [5] studied the cross-sectional surface of the polymer particle using scanning electron microscope; the support fragments decreased in size with increasing prepolymerization yield, and fragmentation of the catalyst was continually progressing during polymerization. Samson et al. [6] found that the highest yields were obtained in lowest prepolymerization temperatures for liquid propylene polymerization; though polymerization rate was mainly determined by the polymerization temperature, besides, heat removal of growing polymer particles became more effective during this stage due to increasing surface area. Tan et al. [7] studied the effect of prepolymerization on the kinetics of propylene bulk polymerization and demonstrated longer isothermal prepolymerization time increased the polymerization rate, especially at the polymerization temperature of 95°C, and the increase in polymerization rate was ascribed to lower intraparticle mass transfer resistances of the internal structure of polymer particles. Tan et al. found that particle size distribution obtained from the nonisothermal prepolymerization was broadest.

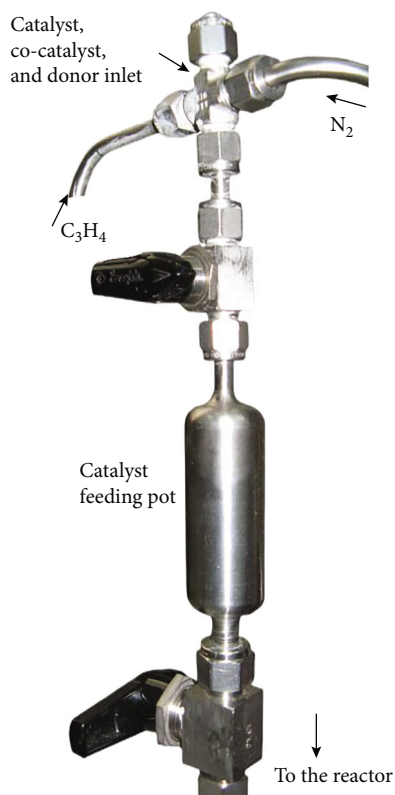


FIGURE 1: Catalyst, cocatalyst, and external donor feeding system.

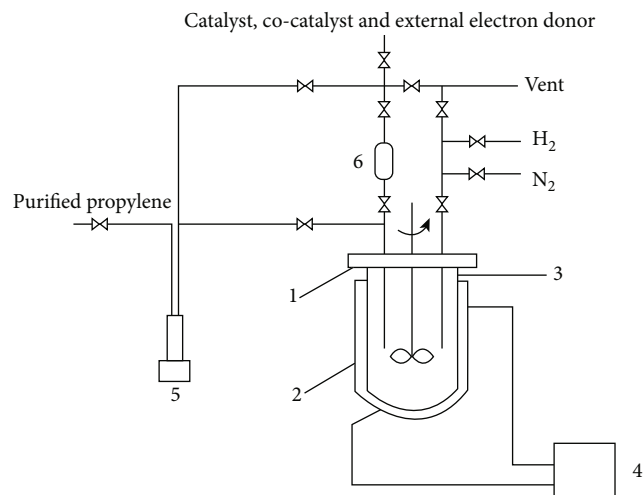


FIGURE 2: Propylene bulk polymerization reactor system: (1) reactor lid, (2) reactor jacket, (3) stainless steel reactor, (4) temperature control system, (5) syringe pump, and (6) catalyst feeding pot.

Monji et al. [8] found that, if the catalyst was prepolymerized at low temperature, both activity and stereoselectivity were improved; besides, the morphology of polymer particles became better. Chen et al. [9] studied the polymerization kinetics of ethylene polymerization and ethylene/1-hexene copolymerization in slurry reactors, and they found that the highest apparent propagation rate constants were achieved using intermediate prepolymerization temperatures, and the

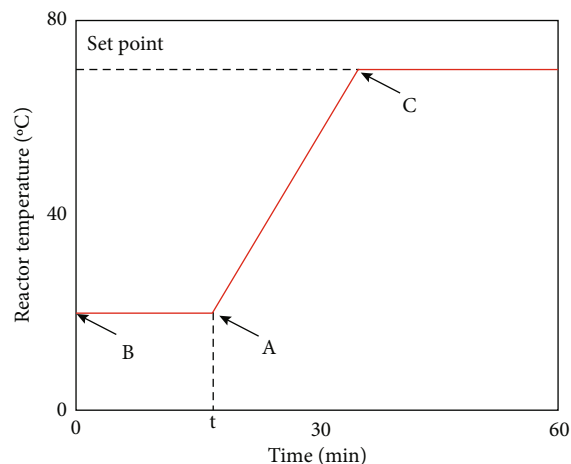


FIGURE 3: Three types of catalyst injection methods: (a) nonisothermal prepolymerization with a catalyst injection at room temperature, (b) isothermal prepolymerization with a catalyst injection at low temperature and keep in this temperature for time t , and (c) isothermal prepolymerization with a catalyst injection at set temperature.

TABLE 1: Conditions for polymerization parallel experiments.

Exp. no.	Catalyst (mg)	Temperature (°C)	Al (mol)/Ti (mol)	Al (mol)/Si (mol)	H ₂ (MPa)
1~2	13.8	70	500	15	0
3~4	10.8	70	500	15	0.030

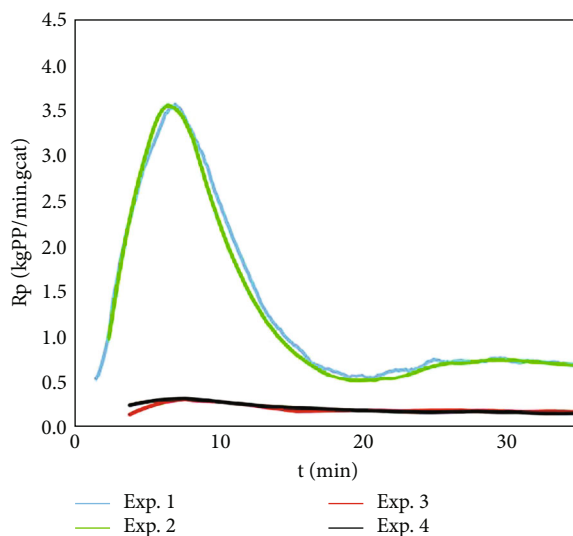


FIGURE 4: Propylene bulk polymerization curves.

apparent deactivation rate constants decreased with increasing prepolymerization temperatures. Chen et al. argued that prepolymer particles with better fragmentation would polymerize at higher rates in the main polymerization reactor.

Usually, prepolymerization was carried out in a slurry reactor, and the prepolymerization yield could be accurately controlled at low temperature. However, little research about propylene bulk polymerization using magnesium alkoxy-

TABLE 2: Conditions and results of propylene bulk polymerization.

Run no.	$t_{\text{prepolymerization}}$ (min)	t_{reaction} (min)	H_2 (MPa)	T ($^{\circ}\text{C}$)	Y (kgPP/gcat)	MFR (g/10 min)	II (%)	$R_{p,0}$ (kgPP/(min·gcat))	k_d (min^{-1})
1	0 ^B , 18 ^A	61	0.120	70	62.3	48.48	93.19	1.691	0.0217
2	0 ^B , 21 ^A	69	0.075	70	65.1	23.13	94.01	1.435	0.0176
3	0 ^B , 15 ^A	61	0.030	80	64.3	7.04	97.46	2.327	0.0287
4	0 ^B , 14 ^A	59	0.030	70	59.0	5.94	95.89	1.883	0.0251
5	0 ^B , 14 ^A	61	0.030	50	16.5	7.56	92.96	0.452	0.0187
6	0 ^B , 18 ^A	61	0.030	60	27.9	7.73	93.95	0.800	0.0207
7	0 ^B , 38 ^A	251	0	70	33.1	0.013	95.29	0.140	0.0047
8	0 ^B , 0 ^A	79	0.030	80	17.2	14.98	94.85	0.516	0.0177
9	0 ^B , 0 ^A	62	0.030	60	18.5	8.74	93.03	0.522	0.0148
10	0 ^B , 0 ^A	77	0.030	50	12.2	14.51	91.52	0.200	0.0078
11	0 ^B , 0 ^A	75	0.120	70	24.3	52.5	89.94	0.541	0.0124
12	0 ^B , 0 ^A	86	0.075	70	38.6	27.53	92.14	0.615	0.0087
13	0 ^B , 0 ^A	60	0.030	70	30.5	8.19	93.98	0.682	0.0108
14	15 ^B , 23 ^A	47	0.030	70	45.1	6.23	95.63	1.436	0.0177
15	30 ^B , 22 ^A	60	0.030	70	56.2	6.96	94.82	1.337	0.0178
16	0 ^B , 0 ^A	60	0.030	90	9.6	26.91	93.33	NA	NA

A: nonisothermal prepolymerization, during this phase, the reactor temperature increases nearly linearly; B: nonisothermal prepolymerization before raising the reactor temperature; $t_{\text{prepolymerization}}$: residence time under different prepolymerization conditions; t_{reaction} : reaction time at polymerization temperature T ; Y : reaction yield of polypropylene per gram of catalyst; $R_{p,0}$: initial polymerization rate obtained by extrapolating the reaction rate curve to time zero; other polymerization conditions: 3 mmol TEA, 0.2 mmol CHMCMS donor.

supported TiCl_4 catalyst was carried out. In this paper, we studied the polymerization kinetics behaviors under different polymerization conditions and the particle size distribution of different prepolymerization time using propylene compensation method and their effects to this simplified prepolymerization process.

2. Experimental Section

2.1. Materials. The polymer-grade propylene (JingHui Gas Company) and nitrogen (99.9%, Sinopec catalyst Co., Ltd. Beijing AODA branch) used in the experiments were added into column packed with molecular sieves to remove H_2O . Hydrogen (>99.999%, JingHui Gas Company) could be used without any purification operation. n-Hexane (99%, Sinopec Beijing Yanshan Petrochemical Company) was purified to remove O_2 and H_2O . Triethylaluminum (TEA, Nouryon Chemicals Co., Ltd.) with a concentration of 10 wt% in hexane was used. Cyclohexyl methyl dimethoxysilane (CHMMS, AR, Shandong Lujing Chemical Technology Co., Ltd.) was used without further purification. The commercial $\text{TiCl}_4/\text{Mg}(\text{OEt})_2/\text{Phthalate ester}$ Ziegler-Natta catalyst [10, 11] (Sinopec catalyst Co., Ltd.) was used in all experiments.

2.2. Catalyst Injection System. The catalyst feeding system is shown in Figure 1. First, the screw cap on the top of the system was twisted under the protection of nitrogen, and the predefined amounts of cocatalyst and external donor were injected into the catalyst feeding pot. Then, the desired amount of catalyst was added into the pot by repeating sucking and discharging the solution in the pot for 5 times to minimize the catalyst loss. When the cap

was screwed and nitrogen feeding was cut off, propylene was added by a syringe pump working at constant-flow mode. When the outlet pressure of the pump was slightly higher than the pressure in the reactor, the valve below the pot was turned on to let the mixture flow into the reactor, and the propylene was kept feeding to make sure that the catalyst, cocatalyst, and external donor were flushed into the reactor totally.

2.3. Reactor System. Polymerizations were carried out in a 3.35 L stainless steel semibatch stirred autoclave reactor, as shown in Figure 2. A precise temperature controlling system was used to adjust the temperature in the reactor at a set value within a deviation of $\pm 0.1^{\circ}\text{C}$. The reactor was equipped with a syringe pump, which was capable of pumping a quantitative volume of liquid propylene into the reactor and kept the reactor pressure constant through continuous compensation of the monomer. The polymerization temperature and pressure were controlled by a DCS system [12].

2.4. Experimental Procedure. Usually, before starting an experiment, the reactor was heated to 110°C , evacuated for 5 min, and refilled with nitrogen. This operation was repeated at least five times to remove trace of oxygen and water in the reactor. When this procedure was completed, the reactor was cooled down to room temperature.

In the experimental stage, a predefined amount of H_2 and liquid propylene was fed into the reactor at room temperature. Next, the reactor is heated to the set temperature about $1\sim 2^{\circ}\text{C}$ lower than the reaction temperature under the stirring speed of 500 rpm, and the desired amounts of catalyst, TEA solution, and external donor (CHMCMS,

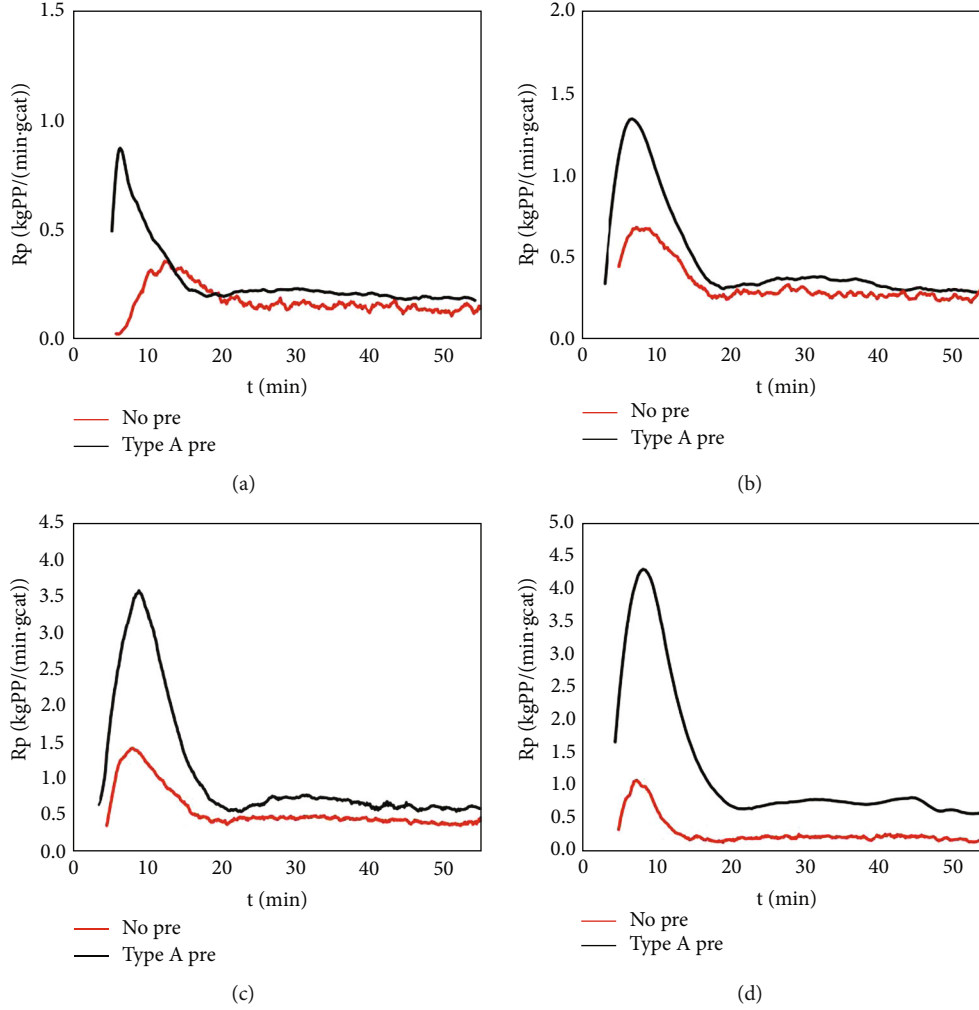


FIGURE 5: Polymerization kinetic curves at different temperatures and the same hydrogen concentration. Black lines: type A catalyst injection; red lines: type C catalyst injection; main polymerization temperature: (a) 50°C, (b) 60°C, (c) 70°C, and (d) 80°C.

0.1 mol/L in hexane) were transferred into the catalyst feed pot under nitrogen pressure. Finally, propylene feed pump at constant-flowrate mode is turned on to flush the catalyst slurry into the reactor. As shown in Figure 3, three different kinds of catalyst injection methods were used in the experiment. When the reactor pressure increases up to the reaction pressure, the pump is switched to constant pressure mode. And then, the reactor is heated to the reaction temperature; meanwhile, three parameters, reactor pressure, reactor temperature, and propylene feed rate, are collected every 6 seconds. To terminate the experiment, the unreacted monomer was flashed off by opening the vent valve.

The reaction rate was calculated from the monomer volume flow fed into the reactor at constant pressure phase. Let $\rho_{m,reactor}$, ρ_{PP} be the density of propylene and polypropylene (PP) in the reactor, respectively, and $V_{m,reactor}$, $V_{PP,reactor}$ be the volume of the monomer and polymer, respectively. Due to volume conservation,

$$\rho_{m,reactor} \frac{\partial V_{m,reactor}}{\partial t} = (\rho_{PP} - \rho_{m,reactor}) \frac{\partial V_{PP,reactor}}{\partial t}. \quad (1)$$

Let m_{cat} be the mass of catalyst injected into the reactor, Q be the monomer volume flow compensated to the reactor and $\rho_{m,pump}$ be the density of monomer in the pump, one can obtain $\partial V_{m,reactor}/\partial t = \rho_{m,pump} Q$. The polymerization rate, R_p (kgPP/gcat-h), can be estimated:

$$R_p = \frac{\rho_{PP} \rho_{m,pump} Q}{(\rho_{PP} - \rho_{m,reactor}) m_{cat}}. \quad (2)$$

2.5. Polymer Characterization. The melt flow rate (MFR) was measured according to ISO 1133 (230°C/2.16 kg).

The isotactic index (II) was determined by conventional chemical extraction using n-heptane according to ISO 9113: 2019.

The particle size and particle size distribution (PSD) were determined by a vibration screener. The polymer particles are cascaded down from the sieve under vibration. The particle size of remaining particles on a particular sieve is defined as the size range between that sieve and the upper sieve.

3. Results and Discussion

3.1. Reproducibility. In order to examine the reliability of the experiment method, two parallel experiments are conducted at 70°C. The same catalyst and external donor (CHMCMS) were used in the experiments, and the ratios of Al (mol)/Ti (mol) and Al (mol)/Si (mol) are also the same. The experimental conditions are listed in Table 1.

Two replicates for propylene bulk polymerization with a nonisothermal prepolymerization phase are shown in Figure 4. The plots of parallel experiments show good agreement, and the deviations observed during polymerization phase are acceptable.

3.2. Estimation of Apparent Kinetic Parameters $R_{p,0}$ and k_d . Ziegler-Natta catalyst is known as a multisite catalyst, and many works showed that multisite model has good agreement for propylene polymerization [13–16]. Despite the complicated nature of Ziegler-Natta catalyst, it can be studied by reducing the types of active sites [17]. Assuming the propagation rate constant and deactivation rate constant are constant during polymerization phase and assuming a first-order deactivation and first-order dependence of the reaction rate on monomer and active site concentration, the simplified model for constant monomer and hydrogen concentrations [1, 3, 18] is

$$R_p = R_{p,0} \cdot \exp(-k_d \cdot t). \quad (3)$$

This equation can be used to fit the isothermal polymerization curve using only initial reaction rate $R_{p,0}$ and deactivation rate constant k_d . It can be assumed that the concentration of catalyst active site reaches the maximum at the very beginning of polymerization due to the reduction rate of catalyst precursor is highly fast.

The experimental conditions and results of propylene bulk polymerization are listed on Table 2. In the experimental group without prepolymerization, the polymerization activity reached the maximum of 30.5 kgPP/gcat·h, and II reached the maximum of 94.85% at 80°C. After nonisothermal prepolymerization, the polymerization activity and isotacticity at 80°C reached the maximum, which were 64.3 kgPP/gcat·h and 97.46%, respectively. For all runs, it can be seen that polypropylene produced with prepolymerization shows higher isotacticity in the main polymerization temperature range of 50–80°C with same hydrogen concentration and Al/Si molar ratio.

3.3. Effort of Polymerization Temperature. Due to the quasisteady-state assumption applied during the initial phase [19–21], the increase in polymerization rate is not real until maximum pressure is reached [22]. During the initial few minutes, in order to keep the reactor pressure constant, overcompensation causes increased pressure of the reactor, leading to the little liquid propylene compensated into the reactor. The polymerization kinetic curves between polymerization with nonisothermal prepolymerization phase and direct isothermal polymerization at different temperatures are compared in Figure 5. At the initial stage of main

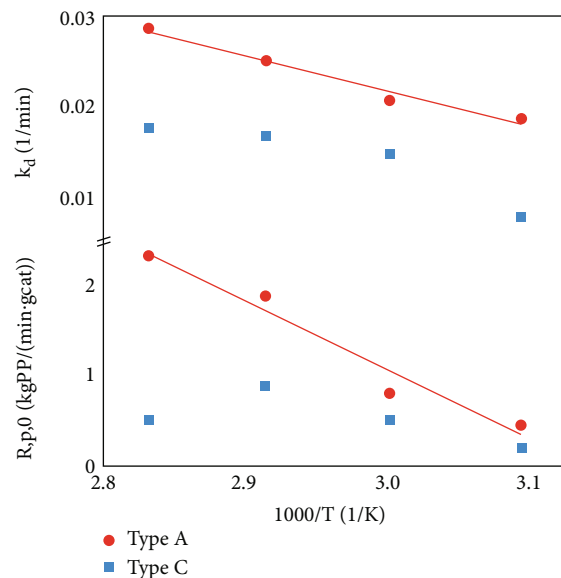


FIGURE 6: Arrhenius plot for the initial reaction rate and deactivation rate constant at different temperatures. Blue square: type A catalyst injection; red dot: type C catalyst injection; the partial pressure of hydrogen was 0.030 MPa.

polymerization, severe flow fluctuation was observed as a consequence of poorly controlled fragmentation and monomer over compensation. The flow fluctuation and temperature fluctuation were levelled off after the reaction rate reached the peak, and only the decay part of polymerization curve known as quasisteady-state zone was applied to fit the profile rate. Nonisothermal prepolymerization improves the morphology of polymer particles and reduces their agglomeration at high temperature; as a consequence, the prepolymerized catalyst particles exhibited better fragmentation and significantly smoothed propylene compensation flow curve. For the polymerization with a catalyst injection at the set temperature, the initial polymerization rate reached the maximum at 70°C and then decreased when polymerization temperature was raised to 80°C, and the polypropylene particles cracked like popcorns at 90°C.

The Arrhenius plot of the initial polymerization rates $R_{p,0}$ (bottom) and the first-order deactivation rate constant k_d (top) at different temperatures are shown in Figure 6. For the polymerization with nonisothermal prepolymerization, the initial polymerization rate increases with increasing temperature. The calculated activation energy is 63.6 kJ/mol for 0.030 MPa hydrogen in the temperature range of 50–80°C. According to activity-dependent probability theory [21], the more monomer converted by active sites, the higher the probability of deactivation. But the deactivation rate constants of runs without prepolymerization did not decrease at 80°C. The polymer accumulates on the surface of the catalyst particles during prepolymerization, which prevented the thermal decomposition of the catalyst caused by overheating. The fragmentation of catalyst is one of the reasons for reaction rate decay, which leads to the increase of catalyst apparent deactivation rate with the increase of temperature. The prepolymerized $\text{Mg}(\text{OEt})_2$ supported catalyst showed

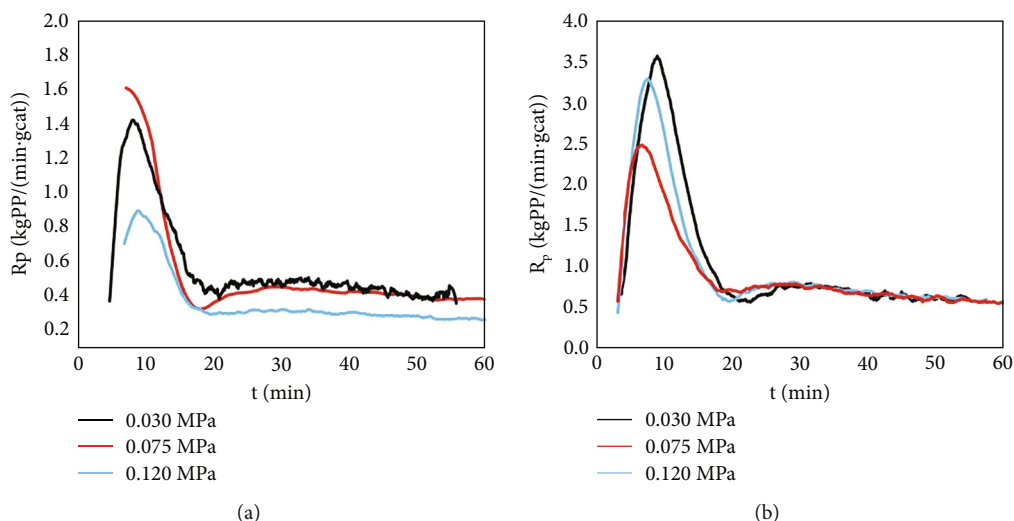


FIGURE 7: Polymerization kinetic curves at different hydrogen pressure at 70°C: (a) type C catalyst injection and (b) type A catalyst injection.

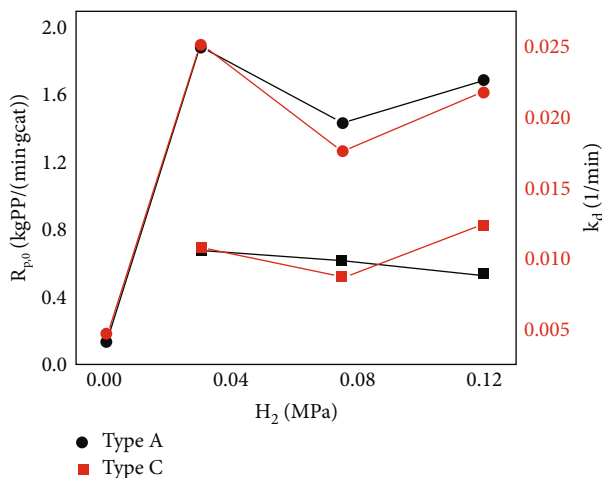


FIGURE 8: Effect of hydrogen partial pressure on polymerization kinetic parameters.

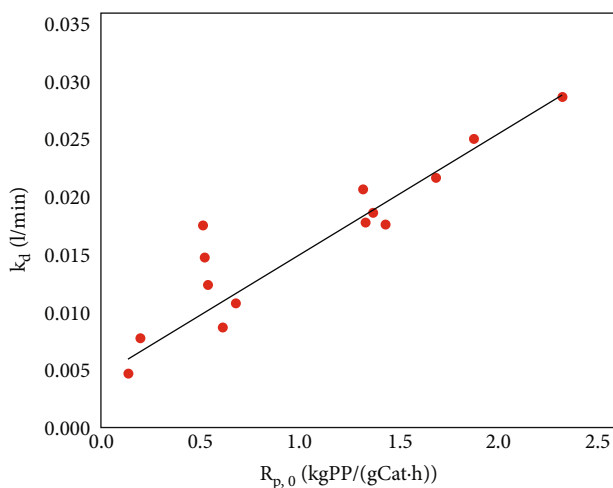


FIGURE 9: Deactivation constant versus initial polymerization rate.

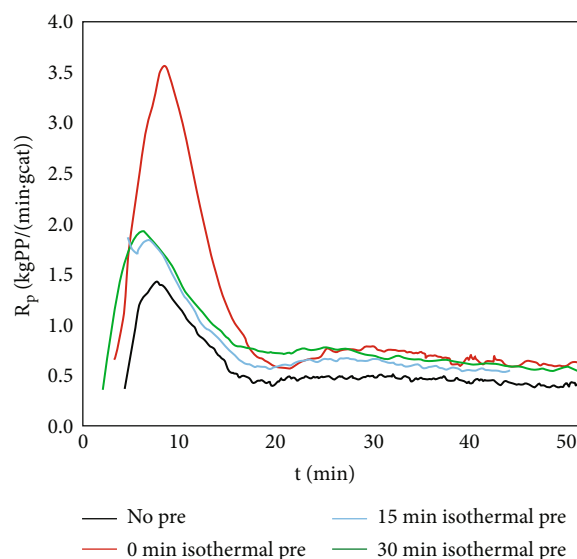


FIGURE 10: Polymerization kinetic curves at varied prepolymerization time.

great difference, and it can maintain high initial polymerization rate and high polymerization activity at high temperature at same time.

At the same hydrogen concentration, the isotactic index of polypropylene tends to increase with the increase of polymerization temperature. Since the more isoselective-active sites produce higher molecular weights polypropylenes [23], the MFR of produced polypropylene would decrease, and polymerization activity would increase with increasing II. The polymerization activity of the group with nonisothermal prepolymerization increased with increasing II, but the MFR increased after the temperature was raised from 70°C to 80°C. The living chain tends to terminate more at 80°C by transfer to hydrogen, and the polymerization activity increases slightly. The results from the group without prepolymerization follow this law in 50°C to 70°C, compare to the

TABLE 3: PSD for polymer produced at varied prepolymerization time.

Fraction (w%)	Bulk density (g/cm ³)	Particle size (μm)							
		2000	1000	500	355	250	180	71	<71
Run 13	0.36	41.05	54.6	3.46	0.18	0.06	0	0.63	0.02
Run 4	0.45	44.95	51.36	3.69	0	0	0	0	0
Run 14	0.45	39.33	54.14	5.25	0.54	0.22	0.04	0.38	0.1
Run 15	0.45	62.52	34.81	2.28	0.14	0.04	0.04	0.17	0

group with nonisothermal prepolymerization, when the temperature raise from 70°C to 90°C, the activity and MFR decreased sharply, and the II decreased mildly. This is caused by mass transfer hindrance and catalyst thermal runaway, and it stands to reason that the influence of mass transfer restriction is more dominating than thermal runaway.

In the group without prepolymerization, the II reaches the maximum at 80°C and decreases slightly at 90°C, while the polymerization activity reaches the maximum value at 70°C and drops sharply at 80°C and 90°C. While the activity of the nonisothermal prepolymerized group kept nearly constant when the temperature increased from 70°C to 80°C, but the II increased significantly. This indicates that the polymerization rate of high-stereoselective active centers increases most with the increase of temperature, and the thermal runaway of high-stereoselective active sites is lower than that of low-stereoselective active centers.

3.4. Effort of Hydrogen. Hydrogen improved the catalytic activity and initial polymerization rate of propylene polymerization, seen in Figure 7, which is usually called activation [24, 25]. It can be explained by hydrogen reactivation of dormant active centers caused by irregular 2,1 insertion [26, 27]. With higher hydrogen concentration, the slope of the rising curve of polymerization rate increases slightly. In the process of olefin polymerization catalyzed by Z-N catalyst, mainly chain transfer reaction and catalyst deactivation several reactions compete with chain propagation. The main chain termination reaction in Z-N catalyst is β -H elimination from the living polymer chain to the metal or β -H transfer of H to monomer, by hydrogenolysis of molecular hydrogen (hydrogen sensitivity) or alkyl transfer to alkyl aluminum [28]. The catalyst used in the experiment is highly hydrogen sensitive, and the polymerization rate does not simply increase with the increase of hydrogen concentration.

The effect of hydrogen partial pressure on polymerization kinetic parameters was shown in Figure 8. The initial polymerization rate and deactivation constant considerably increased as the hydrogen partial pressure was raised from 0 to 0.03 MPa. Both variables declined a little bit when hydrogen was raised from 0.03 MPa to 0.12 MPa. Compared to runs without prepolymerization, both parameters are significantly higher.

The linear relationship between $R_{p,0}$ and k_d for runs with prepolymerization and without prepolymerization were shown in Figure 9. Though the catalyst particles without prepolymerization suffer from thermal runaway, it still satisfies the activity-dependent probability to some extent, indi-

cating that prepolymerization changes the deactivation constant with the same deactivation mechanism.

The addition of hydrogen led to slightly lower stereoselectivity [29] and significantly increased the rate of propylene polymerization and broadened the MWD [30]. Compared to run without hydrogen, the isotactic index of the polymer changed a little when the hydrogen was added. The isotacticity of polymer declined slightly with the increase of hydrogen since higher fraction of low isotactic chains was produced.

3.5. Effort of Isothermal Prepolymerization Time. The polymerization kinetic curves without prepolymerization and with 0, 15, and 30 min isothermal prepolymerization at 20°C were shown in Figure 10. As we expected, runs with prepolymerization exhibit better polymerization rate, and the higher polymerization rate was achieved with less isothermal prepolymerization time. There is 9 min nonisothermal prepolymerization time difference between run 4 and run 14; it turns out this effect is negligible when extrapolating for the initial polymerization rate. The prepolymerized catalyst particles with longer prepolymerization time perform better mechanical strength, but the polymer on the surface will hinder monomer diffuse into the internal catalyst active sites and decrease the polymerization rate.

The polymer particle size distribution (PSD) of the polymer obtained in the experiments was shown in Table 3. Assume the fragmentation rate of catalyst particle is negligible, the size of polymer particles increases with time. Fines generated by the catalyst fragments have few or no active sites with high stereoselectivity, so the fine particles do not grow larger over time. The weight fraction of polymer particles less than 180 μm decreased significantly due to prepolymerization, and the biggest drop occur in run 4. By comparing the fine powder content and polymerization rate, one can reason that the higher polymerization rate was achieved due to less catalyst particle fragmentation, hence less fine generated. Appropriate prepolymerization strategy can effectively reduce the fraction of fine. The fraction of fine increases when the isothermal prepolymerization time increases to 15 minutes; it would decrease again when the isothermal prepolymerization time increase to 30 minutes. Tan et al. reported that a small particle peak appeared in PSD profile at 10 minutes of isothermal prepolymerization, but there is no such phenomenon at 0, 5, and 20 minutes of isothermal prepolymerization [7]. In run 14 and 15, particles less than 180 μm emerged, and the experimental results show certain consistency. The initial polymerization rate and II decrease after extending the isothermal

prepolymerization time; it can be inferred that the polymer accumulated on the catalyst surface grows faster than it is inside at low temperature, resulting in thermal runaway of some fragments with catalyst active sites when the polymer particles were growing.

4. Conclusions

A monomer compensation setup was applied to investigate propene bulk polymerization using a commercial Ziegler-Natta catalyst. We found that the polymerization rate without prepolymerization is small, its polymerization rate reaches the maximum at 70°C, and the isotacticity index reaches the maximum at 80°C. A nonisothermal prepolymerization phase was applied to increase the catalyst stability and polymerization rate, and the initial polymerization rate increased with the increase of temperature. After prepolymerization, the polymerization rate and isotacticity reached the maximum at 80°C, and the polymerization activity reached 1.07 kgPP/(gcat·min). At high polymerization temperature, the mass transfer of monomer inside catalyst was hindered, so the MFR increased with increasing isotacticity index. Prepolymerization improved the stereoselectivity and activity of the catalyst; it showed greater influence on improving mass transfer than preventing catalyst thermal runaway. The content of polymer fine powder obtained with 0 min isothermal prepolymerization was the least.

A simplified model was used to quantify the effect of polymerization conditions on apparent kinetics constants of propylene bulk polymerization. We correlated these changes to the isotactic index and PSD of polypropylene produced. Adequate prepolymerization was capable of increasing initial polymerization rate and reducing the flow fluctuation and the fraction of fine, but increasing the prepolymerization time might reduce the polymerization rate and produce more fine. The initial polymerization rate and deactivation constant increased with the increase of temperature, and it showed good Arrhenius behavior after prepolymerization. The initial polymerization rate and II decreased after extending the isothermal prepolymerization time, which can be explained by worse fragmentation after long prepolymerization time.

Data Availability

The data used to support the findings of this study are included within the supplementary information file.

Conflicts of Interest

The authors declare that they have no conflicts of interest.

Acknowledgments

This work is supported by the SINOPEC science and technology development project (216093).

Supplementary Materials

The supplementary file is the kinetic data of experimental run from 1 to 15. Each run contains two columns, which are divided into polymerization time and corresponding polymerization rate. No. 1-15 stand for run 1-15, respectively. (*Supplementary Materials*)

References

- [1] J. B. P. Soares and T. F. L. McKenna, *Polyolefin Reaction Engineering*, Wiley-VCH, Weinheim, Germany, 2012.
- [2] J. A. Debling and H. W. Ray, "Heat and Mass Transfer Effects in Multistage Polymerization Processes: Impact Polypropylene," *Industrial and Engineering Chemistry Research*, vol. 34, no. 10, pp. 3466-3480, 1995.
- [3] J. T. M. Pater, G. Weickert, and W. P. M. van Swaaij, "Polymerization of liquid propylene with a fourth-generation Ziegler-Natta catalyst: influence of temperature, hydrogen, monomer concentration, and prepolymerization method on powder morphology," *Journal of Applied Polymer Science*, vol. 87, no. 9, pp. 1421-1435, 2003.
- [4] J. T. M. Pater, G. Weickert, and W. P. M. van Swaaij, "Propene bulk polymerization kinetics: role of prepolymerization and hydrogen," *AICHE Journal*, vol. 49, no. 1, pp. 180-193, 2003.
- [5] J. T. M. Pater, G. Weickert, J. Loos, and W. P. M. van Swaaij, "High precision prepolymerization of propylene at extremely low reaction rates—kinetics and morphology," *Chemical Engineering Science*, vol. 56, no. 13, pp. 4107-4120, 2001.
- [6] J. J. C. Samson, G. Weickert, A. E. Heerze, and K. R. Westertep, "Liquid-phase polymerization of propylene with a highly active catalyst," *AICHE Journal*, vol. 44, no. 6, pp. 1424-1437, 1998.
- [7] N. Tan, L. Yu, Z. Tan, and B. Mao, "Microstructure of isotactic polypropylene obtained using Ziegler-Natta catalyst at high polymerization temperature," *Journal of Applied Polymer Science*, vol. 132, no. 36, p. 132, 2015.
- [8] M. Monji, S. Abedi, S. Pourmahdian, and F. A. Taromi, "Effect of prepolymerization on propylene polymerization," *Journal of Applied Polymer Science*, vol. 112, no. 4, pp. 1863-1867, 2009.
- [9] K. Chen, B. Liu, and J. B. P. Soares, "Effect of prepolymerization on the kinetics of ethylene polymerization and ethylene/1-hexene copolymerization with a Ziegler-Natta catalyst in slurry reactors," *Macromolecular Reaction Engineering*, vol. 10, no. 5, pp. 463-478, 2016.
- [10] X. Xiudong, T. Zhong, Y. Lian, and Z. Qilong, "Method for preparing catalyst component, catalyst and application thereof," *CN 105585642 A*, 2016.
- [11] Z. Lan and Y. Lu, "Tailoring morphology and bulk density of magnesium ethoxide particles by adding n-hexane and silicone oil," *Particuology*, vol. 53, pp. 168-174, 2020.
- [12] J. Chen, Y. Du, L. Yu, and Z. Yang, "Bulk polymerization kinetics of propylene with DQC catalyst," *Petrochemical Technology*, vol. 43, 2014.
- [13] Y. V. Kissin, R. I. Mink, T. E. Nowlin, and A. J. Brandolini, "Kinetics and mechanism of ethylene homopolymerization and copolymerization reactions with heterogeneous Ti-based Ziegler-Natta catalysts," *Topics in Catalysis*, vol. 7, no. 1/4, pp. 69-88, 1999.
- [14] L. Zheng-Hong, S. De-Pan, and Y. Zhu, "Multiple active site Monte Carlo model for heterogeneous Ziegler-Natta

- propylene polymerization,” *Journal of Applied Polymer Science*, vol. 115, no. 5, pp. 2962–2970, 2010.
- [15] Z. H. Luo, P. L. Su, D. P. Shi, and Z. W. Zheng, “Steady-state and dynamic modeling of commercial bulk polypropylene process of Hypol technology,” *Chemical Engineering Journal*, vol. 149, no. 1–3, pp. 370–382, 2009.
- [16] Y. P. Zhu, Z. H. Luo, and J. Xiao, “Multi-scale product property model of polypropylene produced in a FBR: from chemical process engineering to product engineering,” *Computers & Chemical Engineering*, vol. 71, pp. 39–51, 2014.
- [17] K. Chen, S. Mehdiabadi, B. Liu, and J. B. P. Soares, “Estimation of apparent kinetic constants of individual site types for the polymerization of ethylene and α -olefins with Ziegler-Natta catalysts,” *Macromolecular Reaction Engineering*, vol. 10, no. 6, pp. 551–566, 2016.
- [18] J. J. C. Samson, P. J. Bosman, G. Weickert, and K. R. Westerterp, “Liquid-phase polymerization of propylene with a highly active Ziegler-Natta catalyst. Influence of hydrogen, cocatalyst, and electron donor on the reaction kinetics,” *Journal of Polymer Science Part A: Polymer Chemistry*, vol. 37, no. 2, pp. 219–232, 1999.
- [19] J. T. M. Pater, G. Weickert, and W. P. M. van Swaaij, “Polymerization of liquid propylene with a 4th generation Ziegler-Natta catalyst—influence of temperature, hydrogen and monomer concentration and prepolymerization method on polymerization kinetics,” *Chemical Engineering Science*, vol. 57, no. 16, pp. 3461–3477, 2002.
- [20] F. Shimizu, J. T. M. Pater, W. P. M. Van Swaaij, and G. Weickert, “Kinetic study of a highly active $MgCl_2$ -supported Ziegler-Natta catalyst in liquid pool propylene polymerization. II. The influence of alkyl aluminum and alkoxy silane on catalyst activation and deactivation,” *Journal of Applied Polymer Science*, vol. 83, no. 12, pp. 2669–2679, 2002.
- [21] M. A. Ali, B. Betlem, B. Roffel, and G. Weickert, “Hydrogen response in liquid propylene polymerization: Towards a generalized model,” *AIChE Journal*, vol. 52, no. 5, pp. 1866–1876, 2006.
- [22] M. A. Ali, B. Betlem, B. Roffel, and G. Weickert, “Estimation of the polymerization rate of liquid propylene using adiabatic reaction calorimetry and reaction dilatometry,” *Macromolecular Reaction Engineering*, vol. 1, no. 3, pp. 353–363, 2007.
- [23] P. C. Barbé, G. Cecchin, and L. Noristi, “The catalytic system Ti-complex/ $MgCl_2$,” in *Catalytical and Radical Polymerization*, Springer, Berlin, Heidelberg, 1987.
- [24] R. Spitz, P. Masson, C. Bobichon, and A. Guyot, “Activation of propene polymerization by hydrogen for improved $MgCl_2$ -supported Ziegler-Natta catalysts,” *Die Makromolekulare Chemie*, vol. 190, no. 4, pp. 717–723, 1989.
- [25] J. B. P. Soares and A. E. Hamielec, “Kinetics of propylene polymerization with a non-supported heterogeneous Ziegler-Natta catalyst—effect of hydrogen on rate of polymerization, stereoregularity, and molecular weight distribution,” *Polymer*, vol. 37, no. 20, pp. 4607–4614, 1996.
- [26] H. Mori, M. Endo, K. Tashino, and M. Terano, “Study of activity enhancement by hydrogen in propylene polymerization using stopped-flow and conventional methods,” *Journal of Molecular Catalysis A: Chemical*, vol. 145, no. 1–2, pp. 153–158, 1999.
- [27] J. C. Chadwick, G. Morini, E. Albizzati et al., “Aspects of hydrogen activation in propene polymerization using $MgCl_2/TiCl_4$ /diether catalysts,” *Macromolecular Chemistry and Physics*, vol. 197, no. 8, pp. 2501–2510, 1996.
- [28] N. Bahri-Laleh, A. Hanifpour, S. A. Mirmohammadi et al., “Computational modeling of heterogeneous Ziegler-Natta catalysts for olefins polymerization,” *Progress in Polymer Science*, vol. 84, pp. 89–114, 2018.
- [29] A. Alshaiban and J. B. P. Soares, “Effect of Hydrogen and External Donor on the Microstructure of Polypropylene Made with a 4th Generation Ziegler-Natta Catalyst,” *Macromolecular Reaction Engineering*, vol. 7, no. 3–4, pp. 135–145, 2013.
- [30] J. B. P. Soares and A. E. Hamielec, “Effect of hydrogen and of catalyst prepolymerization with propylene on the polymerization kinetics of ethylene with a non-supported heterogeneous Ziegler-Natta catalyst,” *Polymer*, vol. 37, no. 20, pp. 4599–4605, 1996.